

# Modeling Arsenic Partitioning in Coal-Fired Power Plants

Constance L. Senior<sup>a,\*</sup>, David O. Lignell<sup>a</sup>, Adel F. Sarofim<sup>a</sup>, Arun Mehta<sup>b,1</sup>

<sup>a</sup>*Reaction Engineering International, 77 W. 200 S. Suite 210, Salt Lake City, Utah 84101, USA*

<sup>b</sup>*EPRI, 3412 Hillview Avenue, Palo Alto, CA 94303, USA*

## Abstract

Vapor-phase arsenic in coal combustion flue gas causes deactivation of the catalysts used in Selective Catalytic Reduction (SCR) systems for  $\text{NO}_x$  control. A one-dimensional model has been developed to predict the behavior of arsenic in the post-combustion region of a coal-fired boiler as a function of gas residence time. The purpose of the model is to calculate the partitioning of arsenic between the vapor phase from volatilization, and arsenic on the ash particles due to surface reaction and/or condensation at temperatures characteristic of SCR systems. The model accounts for heterogeneous condensation of arsenic on the fly ash, as well as surface reaction for two regimes: (1) the free molecular regime (submicron ash particles), and (2) the continuum regime (supermicron ash particles). All gas properties are computed as a function of gas temperature, pressure, and composition, which are allowed to vary. The arsenic model can be used to calculate the impact of coal composition on vapor-phase arsenic at SCR inlet temperatures, which will help utilities better manage coal quality and increase catalyst lifetimes on units operating with SCR. The arsenic model has been developed, implemented, and was tested against experimental data for several coals.

**Keywords:** coal combustion, arsenic, model, SCR poisoning

## 1. Introduction

Selective Catalytic Reduction (SCR) is used to reduce the emissions of oxides of nitrogen from combustion systems. In the SCR process, NO is reduced to  $\text{N}_2$  by injection of ammonia over a catalyst. In coal-fired power boilers, the catalyst is usually based on vanadium oxide supported on titania and is operated at approximately 370 °C. The catalyst activity, the ability of the SCR catalyst to reduce NO, decreases with time in coal-fired boilers. There are several mechanisms by which SCR catalyst activity decreases. One is by reaction with vapor-phase arsenic compounds [1, 2]. Deactivation of SCR catalyst by arsenic has been documented in wet-bottom boilers in which fly ash is reinjected into the boiler, resulting in high concentrations of gaseous arsenic at the SCR inlet [2]. Wet-bottom boilers reject the majority of the ash from the coal in the form of molten slag at the bottom of the combustion chamber. A smaller portion of fly ash leaves the combustion chamber in the flue gas and is subsequently collected in a particulate control device. This fly ash is often reinjected with the fuel, which results in the production of a single solid byproduct stream (slag). In dry-bottom boilers that do not reinject fly ash, arsenic poisoning of SCR catalyst has been less common than in wet-bottom boilers; however,

catalyst deactivation by arsenic poisoning has been noted in dry-bottom boilers as well [3].

Arsenic is presumed to be gaseous  $\text{As}_2\text{O}_3$  or the dimer  $\text{As}_4\text{O}_6$  at SCR temperatures. This molecule is thought to deactivate the catalyst by two mechanisms: blocking micropores in the catalyst, thus preventing NO from reaching active sites, and chemical binding to vanadium oxide sites. Reformulating the catalyst, both chemically and physically, can increase the resistance of the catalyst to arsenic poisoning [1]. Another approach that has been used is to add limestone to the boiler [1, 4]. Calcium oxide reacts with gaseous arsenic oxide upstream of the SCR to form  $\text{Ca}_3(\text{AsO}_4)_2$ , which is the most thermodynamically stable calcium-arsenic compound at conditions typical of coal-fired boilers [4]. Thus, the amount of gaseous arsenic at the SCR catalyst is reduced. Arsenic deactivation of SCR catalysts is not significant if there is sufficient calcium in the coal to react with arsenic in the flue gas. However, there have been instances reported in the literature in which the native calcium content of the coal was too low to provide sufficient protection [3, 4].

In the US, low rank fuels (lignites and subbituminous coals) have sufficient calcium to tie up arsenic in the fly ash. Bituminous coals, however, can have calcium contents that range from 2 wt% to 6 wt% (as CaO in ash). It has been suggested in the literature that CaO in the ash should be greater than 2.5 wt% to minimize poisoning of SCR catalyst by arsenic [3]. Furthermore, the amount of “free” calcium (CaO as opposed to other forms of calcium) is thought to be important [2].

\*Corresponding author. Tel. +801 364 6925; Fax. +801 364 6977  
Email address: senior@reaction-eng.com (Constance L. Senior)

<sup>1</sup>Current address: Pacificorp 1407 W. North Temple, Suite 310, Salt Lake City, UT 84116

## Nomenclature

<i>cfs</i>	Fuchs-Sutugin correction factor (see Eq. 6)	<i>R</i>	universal gas constant
<i>d</i>	ash particle diameter	<i>T</i>	temperature
<i>f</i>	mass fraction	$\lambda$	mean free path in gas
<i>k<sub>o</sub></i>	pre-exponential factor for rate constant	$\mu$	viscosity in gas phase
<i>k<sub>r</sub></i>	rate constant	$\theta$	fraction of arsenic in coal vaporized
<i>np</i>	number of ash particles in a given size bin	$\phi$	mass fraction of submicron ash
<i>t</i>	time	$\rho$	density
<i>A</i>	ash fraction of the active surface area	$\phi$	accommodation coefficient, fraction of successful collisions with the particle surface
<i>C</i>	concentration of arsenic (g/g)	<b>Subscripts</b>	
<i>D</i>	gas-phase diffusivity	<i>a</i>	ash property
<i>E<sub>act</sub></i>	activation energy	<i>c</i>	coal property
<i>F<sub>i</sub></i>	flux of arsenic to a particle of size i	<i>f</i>	final
<i>Kn</i>	Knudsen number, 2/d	<i>i</i>	particle size bin
<i>M<sub>As<sub>4</sub>O<sub>6</sub></sub></i>	moles of As <sub>4</sub> O <sub>6</sub> in gas phase	<i>o</i>	initial
<i>MW</i>	molecular weight, g/mol	<i>s</i>	conditions at particle surface
<i>P</i>	vapor pressure	$\infty$	conditions in bulk gas

The behavior of arsenic in a furnace is dependent upon the amount of arsenic vaporized during combustion and its subsequent interactions with gas-phase species and ash particles. Arsenic in coal occurs primarily in the mineral inclusions, as opposed to the organic fractions [6]. Arsenic in coal is primarily associated with pyrite/sulfides where it substitutes for sulfur in the pyrite structure. For bituminous coals, typically up to about 15% of arsenic is contained in silicate fractions. Arsenic has a relatively high volatility, and the fraction not associated with silicates (which have high vaporization temperatures) is expected to volatilize. The oxidation states of arsenic are +3 and +5, and volatilized arsenic is expected to oxidize to form gaseous  $\text{As}_4\text{O}_6$ . This species then interacts with the ash in the post-combustion flue gas, dependent upon the size and composition distribution, along with the gas temperature profile.

Only trace concentrations of arsenic are found in coal, typically 2 to 20  $\mu\text{g/g}$ . Figure 1 shows gaseous arsenic concentrations from three wet-bottom boilers measured at the first catalyst layer of the SCR, that is at temperatures of  $\sim 370^\circ\text{C}$  [2]. These boilers recycled fly ash back into the boiler, which served to drive up the vapor-phase arsenic concentration at the SCR. As the figure shows, the addition of limestone reduced the vapor-phase arsenic at the SCR by about two orders of magnitude, presumably by the reaction between vapor-phase arsenic and calcium oxide to form  $\text{Ca}_3(\text{AsO}_4)_2$ . There are two possible paths

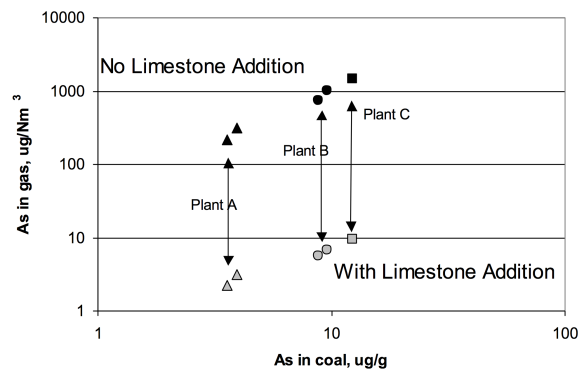


Figure 1: Measured arsenic concentration at first catalyst layer (in  $\mu\text{g}/\text{Nm}^3$ ) as a function of coal arsenic content. Data of Pritchard et al. [2] shown for wet-bottom boilers with 100% fly ash recycle, with and without limestone injection for three different plants.

for arsenic removal from the vapor: heterogeneous condensation, and surface reaction on the ash particles. It is well known that ash forms a bimodal size distribution, with submicron particles formed as part of the ash that is vaporized in the high temperature burning coal char, and that later condenses in cooler regions, and supermicron particles from residual ash agglomeration. The submicron size range is important since the majority of the ash surface area resides in this regime, although most of the ash mass is contained in the larger fraction. This is discussed more below.

In this paper, we develop a model for the gas-to-solid conversion of arsenic in coal-fired boiler exhaust gases. This is a one-dimensional model that includes condensation and reaction with calcium with vapor-phase arsenic on the fly ash as temperatures decrease in the post-combustion section of the boiler. The model takes into account the available surface area of calcium in the fly ash as well as the competition between arsenic and sulfur for calcium surface sites. The model is intended to predict the concentration of arsenic in the vapor phase at the inlet to the SCR. The model is validated against pilot-scale data for partitioning of arsenic in fly ash from combustion of six different coals. The model can be used to examine the impact of coal composition on catalyst activity.

## 2. Model Description

### 2.1. General Flux Equations

This section describes the equations used to develop the arsenic partitioning model. Heterogeneous condensation of  $\text{As}_4\text{O}_6$  on ash particles is based on equilibrium between the vapor- and condensed-phase species. The surface reaction mechanism is primarily between the gaseous arsenic species, which can form an oxy-anion ( $\text{AsO}_4^{3-}$ ) in the condensed phase, and cationic species, primarily calcium. Because ash particles are non-porous and spherical, the reaction rate is dependent only on the particle size, the arsenic concentration, the fraction of the active surface area (calcium content), and an Arrhenius-based reaction rate constant.

The model is one-dimensional in time and consists of specifying the initial condition of the system: flue gas composition, initial gas temperature, vapor-phase arsenic concentration, and initial particle arsenic concentration. The initial arsenic concentration on the ash particles is computed assuming zero concentration for all submicron particles, which are assumed to be formed from ash vaporization followed by homogeneous condensation and agglomeration. Arsenic not vaporized is assumed to be uniformly distributed on the supermicron ash particles. If the initial arsenic concentration on a given size is assumed proportional to the concentration of another compound in the ash particle, say compound “B”, then the following equation

would apply:

$$C_{o,i} = \frac{(1-\theta)}{f_a} \frac{(C_B)_i}{\sum_i (C_B)_i f_i}, \quad (1)$$

where  $(C_B)_i$  is the concentration of compound  $B$  in g/g ash,  $f_i$  is the mass fraction of ash size  $i$ ,  $\theta$  is the fraction of arsenic in coal vaporized,  $f_a$  is the mass fraction of ash in the coal,  $C_c$  is the concentration of arsenic in coal (g/g), and the summation is taken only over supermicron particles. For uniform  $C_B$ , Eq. 1 reduces to:

$$C_{o,i} = \frac{(1-\theta)}{(1-\phi)} \frac{C_c}{f_a}, \quad (2)$$

where  $\phi$  is the mass fraction of submicron ash. This equation assumes a uniform distribution of arsenic on the supermicron particles.

The vapor-phase arsenic is transported to the particle surface where it interacts by one of two mechanisms: physical condensation and surface reaction. These mechanisms are computed as fluxes, with units of moles  $\text{As}_4\text{O}_6$  per second per particle. We do not assume that both mechanisms occur at the same time as discussed below. The equations for each mechanism depend on the gas-phase transport regime: free molecular (submicron) or continuum (supermicron). Thus, four flux equations are used to describe the transport.

The concentration of arsenic on a given ash particle at a given time  $t_f$  is given by the following equation,

$$C_i = C_{o,i} + \frac{4MW_{\text{As}}}{\frac{\pi}{6}\rho_i d_i^3} \int_{t=0}^{t=t_f} F_i(t) dt. \quad (3)$$

Here,  $\rho_i$  and  $d_i$  are the ash particle density and diameter, respectively, which are both assumed constant. The total particle mass is also assumed constant, since the total mass of arsenic is much less than the mass of the ash particle. Arsenic concentrations are measured in  $\mu\text{g}/\text{g}$ . The factor of 4 converts between moles of  $\text{As}_4\text{O}_6$  and moles of elemental arsenic, which is used in defining the arsenic particle concentration. Equation (3) is integrated numerically for each particle size, allowing for changing gas and transport properties with time.

At each time step, the moles of  $\text{As}_4\text{O}_6$  removed from the flue gas are computed as

$$\Delta M_{\text{As}_4\text{O}_6} = \sum_{i=\text{sizes}} F_i n p_i \Delta t, \quad (4)$$

where  $F_i$  is the flux for the given size, referred to above, and defined below, and  $n p_i$  is the number of ash particles of size  $i$  for our given basis of 1 gram of coal.  $n p_i$  is computed as

$$n p_i = \frac{f_a f_i}{\frac{\pi}{6} \rho_i d_i^3}. \quad (5)$$

The following equations are used to describe the flux of  $\text{As}_4\text{O}_6$  to the particle surfaces.

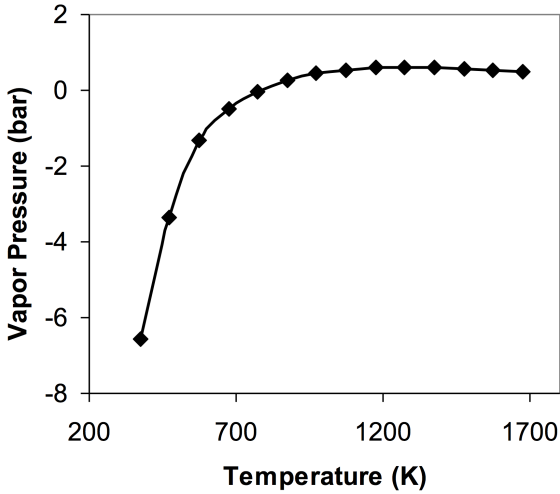


Figure 2: Equilibrium vapor pressure of  $\text{As}_4\text{O}_6$  (g).

## 2.2. Heterogeneous condensation, continuum regime

The equation used to describe the condensation flux in the continuum regime is given by:

$$F_i = \frac{2\pi d_i D}{RT} (P_\infty - P_s) \left[ \frac{1 + Kn}{1 + 1.71Kn + 1.33Kn^2} \right], \quad (6)$$

where  $Kn = 2\lambda/d_i$  is the Knudsen number,  $D$  is the diffusivity of  $\text{As}_4\text{O}_6$ ,  $P_\infty$  and  $P_s$  are the bulk and surface pressures of  $\text{As}_4\text{O}_6$ , respectively. The term in brackets in Eq. (6) is the Fuchs-Sutugin correction (cfs) for the non-continuum behavior of small particles. For large particles the term becomes unity. The mean free path  $\lambda$  is computed as

$$\lambda = \frac{\mu}{\rho} \left( \frac{\pi MW}{2RT} \right)^{1/2}, \quad (7)$$

where the molecular weight, viscosity and density of the gas are calculated using the overall gas composition. The diffusivity of  $\text{As}_4\text{O}_6$  is computed using the empirical equation of Fuller, Schettler, and Giddings [7], which utilizes atomic diffusion volumes. The correlation provides a means of computing a molecules diffusivity based on its atomic components. Since arsenic was not in the list of elements with diffusion volumes, its diffusion volume was extrapolated by correlating atomic radius (known for all elements) with diffusion volume for the eight elements that were provided. The correlation was a good one and the arsenic oxide diffusivity was reasonable. The surface pressure,  $P_s$  is computed as the equilibrium vapor pressure of the gas in the following reaction:  $2\text{As}_2\text{O}_3$  (s) =  $\text{As}_4\text{O}_6$  (g). Figure 2 shows a plot of the vapor pressure versus temperature. The relatively high vapor pressure at low temperature implies condensation will only occur at very low temperatures and relatively high concentrations of arsenic in the vapor-phase.

## 2.3. Heterogeneous condensation, free molecular regime

The flux in the free molecular regime (submicron particles) is given by

$$F_i = \frac{\psi \pi d^2 (P_\infty - P_s)}{(2\pi M W R T)^{1/2}}, \quad (8)$$

where  $\psi$  is the accommodation coefficient, or the fraction of successful collisions with the particle surface, taken as unity.

## 2.4. Surface reaction, continuum regime

The flux equation for the surface reactions is given by the following equation:

$$F_i = \frac{2\pi d_i}{RT} \left[ \frac{P_\infty}{\frac{2}{d_i k_r A} + \frac{1}{D cfs}} \right], \quad (9)$$

where  $k_r$  is the reaction rate constant in units of (m/s), and  $A$  is the fraction of the active surface area, where reactions are assumed to occur between the  $\text{As}_4\text{O}_6$ , which is an oxy-anion, and calcium cations at the particle surface.  $A$  is assumed equal to the mass fraction of CaO in a given ash size. Equation (9) is written in terms of the bulk arsenic partial pressure, rather than the surface pressure, so the diffusive resistance is added to the reactive resistance in the denominator of the term in brackets. The corresponding surface pressure for the reaction only is computed by

$$P_s = \frac{2DP_\infty}{2D + dk_r A}. \quad (10)$$

## 2.5. Surface reaction, free molecular regime

The reaction flux for the free molecular regime is given by

$$F_i = \frac{\pi d^2}{RT} k_r P_\infty A. \quad (11)$$

For the free molecular regime, there is no diffusion resistance, and the surface pressure is equal to the bulk pressure.

The reaction fluxes presented are not expected to occur in parallel, rather, only heterogeneous condensation or surface reaction occurs, depending on the conditions. For temperatures above 1200 °C, neither mechanism will occur. As discussed above, if the equilibrium vapor pressure is greater than the bulk partial pressure, the heterogeneous condensation flux is assumed zero; negative values are not allowed. For the surface reactions, if the surface pressure, Eq. (10) (or the bulk pressure for the free molecular regime) is greater than the equilibrium vapor pressure, the reaction fluxes are assumed zero, and only heterogeneous condensation occurs. The reaction rate constant is based on measurements by Helble and co-workers of the uptake of vapor generated from arsenic trioxide by samples of CaO or calcium silicate suspended in a microbalance [6]. Data on weight gain were collected from 800 °C to 1500

°C. These were used to compute a pre-exponential factor,  $k_o$  and an activation energy,  $E_{act}$ . This  $k_r$  has the form:

$$k_r = k_o e^{-E_{act}/RT}. \quad (12)$$

The activation energy for reaction of calcium silicate and vapor from arsenic trioxide in an oxidizing environment was computed by Helble and coworkers from measurements as 19.3 kJ/mol [6]. In the present work, the pre-exponential factor,  $k_o$ , was selected to be 8.8 (m/s), a value that gave the best agreement between the surface reaction and pilot-scale data on arsenic distribution in ash.

### 2.6. $SO_2$ effects

The sulfur present in flue gas is able to react with calcium in ash to reduce the reactivity of the ash towards arsenic, resulting in reduced arsenic capture. The reaction occurs primarily between  $SO_2$  and CaO to form calcium sulfite ( $CaSO_3$ ), which then oxidizes to form calcium sulfate. This important effect is included in the model. All the sulfur in coal is assumed to form  $SO_2$ , and the  $SO_2$  flux is computed using the flux equations for surface reaction, as for arsenic, listed in Eqs. (9) and (11). In these equations, the diffusivity and partial pressure of  $SO_2$  replace those of arsenic oxide. The rate constant is computed from the Arrhenius equation,  $k_r = k_o * \exp(-E_a/RT)$  with  $k_o = 1.07 \text{ moles/s}^* \text{m}^2 * \text{Pa}$ , and  $E_a = 141.3 \text{ kJ/mol}$  [8]. The rate constant is multiplied by a factor of  $R * T$  to give units of m/s, as compatible with the rate constant presented in Eqs. (9) and (11).

### 2.7. Computer model flow diagram

A computer program was written to compute the arsenic flux to ash particles, given an initial coal composition and a time-temperature history. Figure 3 shows a flow diagram for the computer model developed. The inputs to the model can be split into three groups: (1) flue gas composition and time-temperature profile, (2) ash size distribution and properties, and (3) initial arsenic concentration, and speciation. In order to compute the arsenic partitioning, the composition and time versus temperature profile of the flue gas are required. The flue gas composition is obtained by specifying the coal ultimate analysis (C, H, O, N, S, Cl, Ash, Moisture), the combustion air composition, and the stoichiometric ratio, assuming complete combustion. The time-temperature profile is input directly. A basis of one gram of as-received coal is taken as a basis for the calculation. For input group two, the post-combustion ash size distribution is specified as particle diameter versus mass fraction. In addition, ash density and calcium content for each size are specified. The group three inputs require the arsenic concentration in the coal and fraction of arsenic volatilized during combustion. Because the arsenic is present in only trace quantities in the coal, typically on the order of 10 µg/g, the volatilized arsenic as  $As_4O_6$  is added to the flue gas directly, without regard to the material balance defined by the group 1 inputs. The  $As_4O_6$  in the flue gas will be on the order of 1 ppmv or less.

## 3. Experimental data

### 3.1. Pilot-scale data

Experiments were carried out at the University of Arizona pilot-scale combustor [9]. This is a vertical, down-fired furnace, 6 m tall and 0.15 m internal diameter, that is designed to simulate the time-temperature histories and complex particle interactions of commercial-scale combustors. Combustion is self-sustained in the refractory-lined furnace; all experiments were carried out under lean conditions with 20% excess air. Six different coals were burned in the pilot-scale furnace. Table 1 gives the compositions of the coals.

Isokinetic particle sampling was performed from the centerline of the furnace using a water-cooled, aspirated probe. The sampled gases were quenched and diluted with nitrogen in order to stop chemical reactions and condense any vapor species with dewpoints above room temperature. A Berner-type low pressure impactor [10] was used to collect size-segregated samples. This impact has seven stages with cutoff diameters less than 1 micron and the smallest stage has a cutoff diameter of 0.0324 µm.

The ash size distribution is critical in modeling the arsenic partitioning in the post-combustion flue gases. The important mechanisms for arsenic partitioning to fly ash are surface reaction and heterogeneous condensation between the vapor-phase arsenic species and the ash particles. These two mechanisms strongly depend on the particle size distribution. Hence, the particle size distribution is important.

Figure 4 and Table 2 give the ash size distributions for six coals. The well-known bimodal size distribution of ash is evident in the figure. The peak at small sizes is due to the vaporization of part of the ash in the high temperature burning char. As the gases cool, the ash vapor is supersaturated, condenses and then agglomerates homogeneously to form an ash fume. The second, larger peak is from the residual ash particles. The ash size distribution is taken as a user-input into the arsenic model, with defaults provided, and values given here can be used directly.

Table 3 shows the mass fraction and surface area fractions of the ash particles below one micron. These values are important since the arsenic calculations are carried out for the sub- and super-micron particles separately. Note that while most of the particle mass resides in the large particles, the bulk of the particle surface area resides with the submicron particles. Nearly 100% of the particle number density resides in the submicron particles.

### 3.2. Arsenic vaporization

The fraction of the arsenic that vaporizes in the combustion zone is a critical input parameter for the calculation of post-combustion arsenic partitioning. Using data from the DOE program for assessment of air toxics from power plants [11, 12, 13, 14, 15, 16, 17, 18, 19], the amount of arsenic vaporization was calculated at eight different power plants from the concentrations of arsenic in the coal

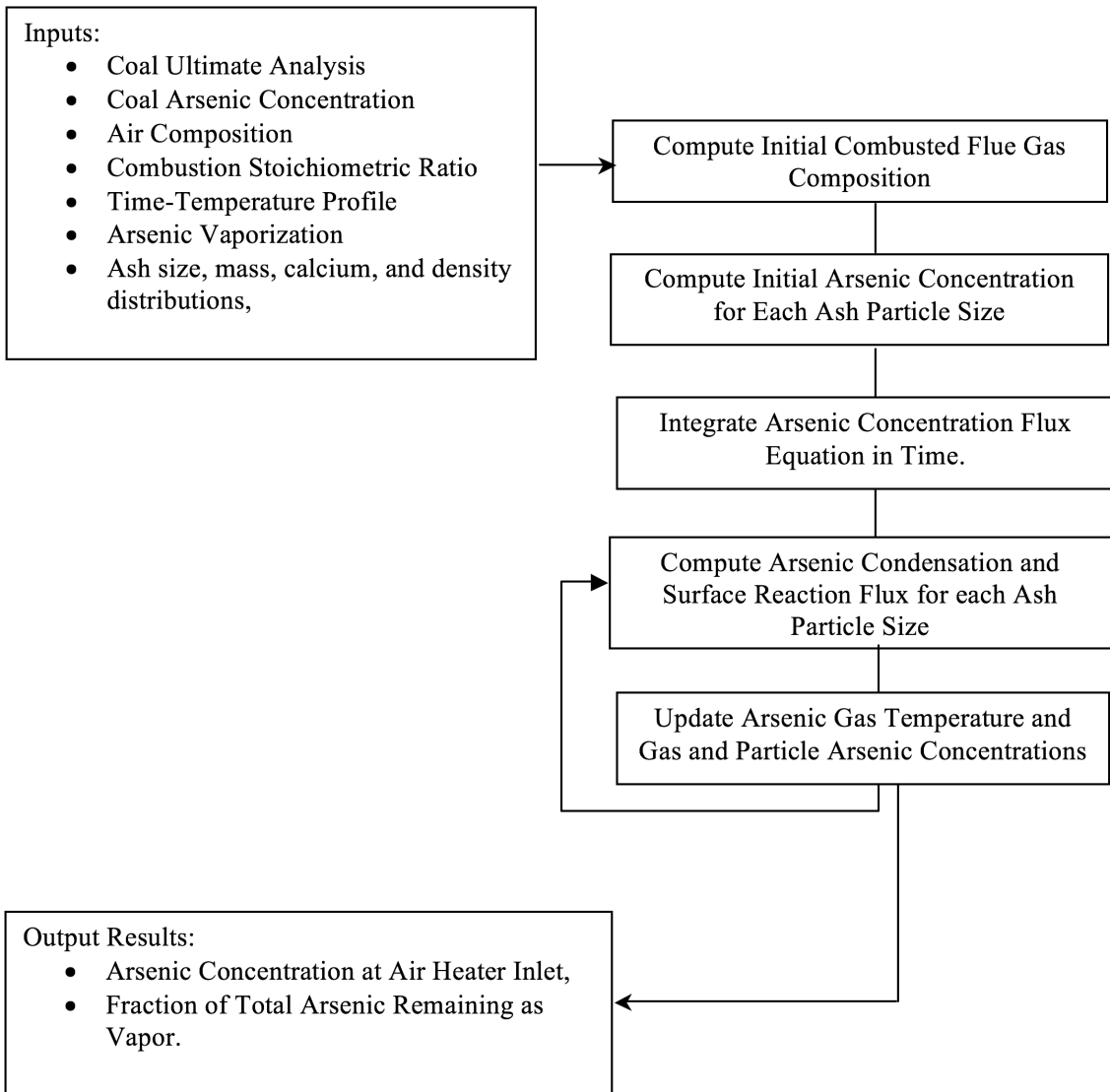


Figure 3: Arsenic model flow diagram.

Table 1: Composition of six coals burned in pilot-scale combustor [9].

	Illinois Bitum.	Pittsburgh Bitum.	Ohio Bitum.	Kentucky Bitum.	Wyodak Subbit.	North Dakota Lignite
Ultimate Analysis (wt%)						
C	67.70	76.62	69.41	74.87	37.98	28.62
H	4.73	4.80	4.95	4.59	4.83	4.89
N	1.18	1.48	1.34	1.43	0.53	0.31
S	3.60	1.64	2.56	0.82	0.24	0.47
O	9.50	6.91	9.93	8.38	26.14	32.95
Moisture	3.31	1.44	2.33	2.33	25.81	25.81
Ash	10.26	7.01	9.47	7.41	4.47	6.96
As in coal, $\mu\text{g/g}$	2.70	4.10	19.00	4.00	1.40	8.10
Ca/S (g/g coal)	0.2786	0.4598	0.1690	0.1775	3.6329	3.1067
Ca/As (g/g coal)	10,588	7,862	843	3,288	116,087	26,691

Table 2: Post-combustion ash size distribution (%) for six coals.

Size ( $\mu\text{m}$ )	Illinois Bitum.	Pittsburgh Bitum.	Ohio Bitum.	Kentucky Bitum.	Wyodak Subbit.	North Dakota Lignite
0.0324	0.95	0.76	0.30	0.23	1.10	0.57
0.0636	0.53	1.54	0.90	0.16	1.21	0.90
0.0926	0.56	1.02	0.55	0.13	3.34	1.31
0.168	0.69	1.17	0.28	0.15	3.89	1.38
0.337	1.09	2.01	0.08	0.40	2.47	1.78
0.535	4.99	5.90	0.18	0.76	6.64	2.79
0.973	11.45	7.83	7.98	8.20	12.02	3.45
1.96	6.07	10.34	28.52	14.39	21.07	10.79
3.77	12.76	12.55	16.50	21.15	16.16	22.60
7.33	46.25	50.27	32.64	39.33	22.58	47.12
15.7	14.66	6.61	12.07	15.12	9.53	7.33

Table 3: Submicron ash particle mass and area fractions for six coals.

	Illinois Bitum.	Pittsburgh Bitum.	Ohio Bitum.	Kentucky Bitum.	Wyodak Subbit.	North Dakota Lignite
wt % in submicron ash	20.3	20.2	10.3	10.0	30.7	12.2
surface area % in submicron ash	84.0	85.1	62.2	54.1	88.5	78.7

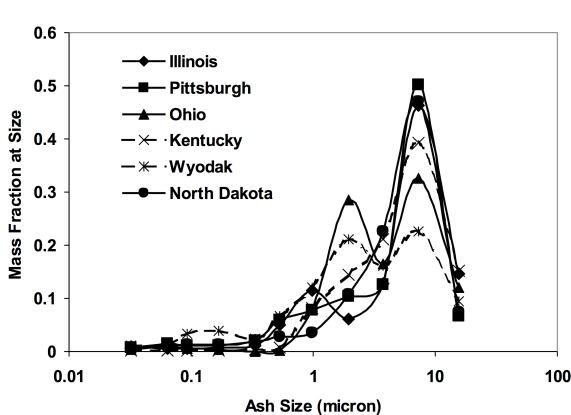


Figure 4: Post-combustion ash size distribution for six coals.

and bottom ash. The concentration of the arsenic in the bottom ash represents the portion of arsenic that does not enter the vapor phase in the combustion zone. The arsenic vaporization calculated in this way is not influenced by or related to any condensation of vapor-phase arsenic on fly ash subsequent to the combustion zone.

Table 4 summarizes the arsenic mass balances and arsenic partitioning taken from the full-scale measurements. The arsenic vaporization thus calculated varies from 55% to 98%. Coal rank and furnace type are both important, according to Table 4 and Fig. 5. Arsenic vaporization is higher for higher coal ranks, but this effect is primarily a function of flame temperature, as indicated by the higher arsenic vaporization in cyclone boilers as compared to tangential boilers.

The degree of arsenic vaporization in the pilot-scale facility [9] was estimated from the normalized experimental arsenic concentration on the largest ash sizes, which have the smallest vapor-phase arsenic flux. The initial arsenic concentration of particles less than 0.1  $\mu\text{m}$  is assumed to be zero, since this ash is assumed to originate from condensation of vaporized ash. In the data of Seames, the experimental values of the concentration of arsenic in ash did not satisfy a material balance based on the coal composition. Therefore, the experimental ash concentrations were normalized assuming 100% capture of vaporized arsenic by ash. The resulting calculations of arsenic vaporization are given in Table 5. The calculated vaporization agrees

Table 4: Characteristics of full-scale plants.

Boiler type	Capacity MWe gross	Coal	Sulfur in coal, wt% dry basis	%Ash in coal	Calcium, coal $\mu\text{g/g}$ dry	Arsenic, coal $\mu\text{g/g}$ dry	Ca/As coal ratio	Arsenic, Bottom Ash $\mu\text{g/g}$	As Mass Balance %	Frac. As Vap.
Cyclone	345	Bitum.	3.5	11.96	3602	3.1	1145	0.35	84.4	0.987
Cyclone	568	Bitum.	3.4	12.04	4939	3.1	1588	1.26	81.05	0.951
Cyclone	108	Bitum.	2.8	11.9	—	35.7	—	6.43	52.7	0.979
Cell Burners	615	Bitum.	3.2	11.36	307	12.8	24	23.00	—	0.796
Wall	69	Subbit.	0.9	11.16	7374	1.8	4067	3.583	74.4	0.780
Tangential	100	Bitum.	2.7	11.1	2141	2.3	917	7.15	270	0.659
Tangential	397	Subbit.	0.7	23.48	5046	3.1	1644	3.36	81.5	0.743
Tangential	1100	Lignite	1.0	16.6	—	7.6	—	20.7	52.9	0.552

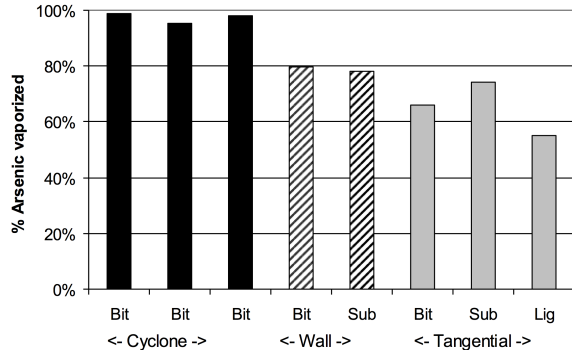


Figure 5: Arsenic vaporization from DOE Toxics Assessment program [6] as a function of boiler type and coal rank.

with the full-scale data and ranges from 36% to 95%. As observed in full-scale data, the amount of vaporization is higher for bituminous coals as compared to low rank coals.

#### 4. Results

Time-temperature histories taken from Seames [9] were used along with the coal and ash information previously discussed to calculate the distribution of arsenic in the ash as a function of size for all six coals. Table 5 lists the experimental residence time, peak temperature measured in the furnace, the temperature at the sampling point and the estimated arsenic vaporization used in the model. In addition, Table 5 compares the calculated amount of arsenic partitioning with the measured amount of arsenic partitioning.

Figure 6 compares the measured and predicted arsenic concentrations in the ash as a function of particle diameter. The model correctly predicts trends in the experimental data and does a good job of predicting the amount of arsenic in the submicron particles. In the ultrafine (less than  $0.1 \mu\text{m}$ ) size, however, the model did not do as good

a job for some of the bituminous coals. The experimental CaO distributions for Illinois and Pittsburgh coals are suspect, since only two minerals in ash were reported for these coals. Coals with low capture of vapor-phase arsenic by ash (Ohio and Kentucky) show much lower concentrations than the experimental data assuming 100% conversion of arsenic to ash.

Coals with high Ca/As ratios and low sulfur (Wyodak and North Dakota), show significant enrichment of arsenic in small sizes and high recovery of vapor to ash. Due to the relatively high vapor pressure of  $\text{As}_4\text{O}_6$  and to the low concentration of arsenic in the vapor, no physical condensation is expected.

It was observed in the pilot-scale study that there were effects of sulfur concentration and calcium on arsenic speciation. The sensitivity of arsenic partitioning to these factors was tested by running cases for the six coals described above using a single temperature profile for a typical boiler (Fig. 7) in which the temperature varied from  $1317^\circ\text{C}$  to  $370^\circ\text{C}$  in 2.5 s. ( $370^\circ\text{C}$  is a typical air preheater inlet temperature.) An average arsenic vaporization rate of 75% was assumed for all coals. We used the size and calcium distribution profiles for each coal from Seames [9].

The baseline results, using the inputs described above, are given in Table 6 in terms of the amount of arsenic in the vapor phase at  $370^\circ\text{C}$ .

Figures 8 and 9 illustrate the effect of sulfur on the predicted size distribution of arsenic in the ash and on the predicted vapor-solid partitioning at SCR inlet temperatures for the Pittsburgh and Kentucky coals, respectively. Sulfur, in the form of gaseous  $\text{SO}_2$  has a large effect on the amount of arsenic in the submicron ash, particularly the ultrafine ash less than  $0.1 \mu\text{m}$ . The ultrafine ash has a high specific surface area and, for most of the coals, relatively high concentrations of calcium. The calcium reacts preferentially with  $\text{SO}_2$ , so as the amount of  $\text{SO}_2$  in the flue gas increases, the amount of arsenic in the ultrafine ash

Table 5: Conditions for vaporization calculations and comparison of measured and calculated arsenic partitioning in ash for pilot-scale combustion experiments.

	Illinois Bitum.	Pittsburgh Bitum.	Ohio Bitum.	Kentucky Bitum.	Wyodak Subbit.	North Dakota Lignite
<b>Experimental conditions</b>						
Residence Time to Sampling Point (s)	3.5	2.9	3.2	2.9	6.6	9.44
Peak Flame Temperature (°C)	1292	1292	1357	1387	1197	1152
Sampling Temperature (°C)	792	792	797	947	687	596
<b>Quantities calculated from data</b>						
% As Vaporization in Flame	72.6	94.8	77.7	62.9	56.3	36.3
% As Captured by Fly Ash	37.9	37.2	14.1	5.7	100.0	100.0
% As in Fly Ash < 1 μm	44.3	94.3	59.8	24.4	54.1	26.1
% As in Fly Ash < 0.1 μm	0.9	1.3	2.6	2.3	16.2	7.3
<b>Quantities predicted by model</b>						
Conc. As in Flame (ppbv)	16.3	29.2	111.1	19.6	11.0	55.8
Conc. As at Sampling Pt. (ppbv)	10.2	18.4	95.0	18.5	0.0	0.0
% As in Fly Ash < 1 μm	47.6	83.6	20.7	12.5	60.6	32.4
% As in Fly Ash < 0.1 μm	9.5	23.3	1.9	2.1	38.6	17.3

Table 6: Predicted vapor-phase arsenic concentrations for six coals, assuming the full-scale boiler time-temperature history in Fig. 7.

	Illinois Bitum.	Pittsburgh Bitum.	Ohio Bitum.	Kentucky Bitum.	Wyodak Subbit.	North Dakota Lignite
As <sub>4</sub> O <sub>6</sub> Conc. in Flame, ppbv	17	23	107	23	15	115
As <sub>4</sub> O <sub>6</sub> Conc. at 370 °C, ppbv	12	15	96	22	0	1
Percent of As in Ash at 370 °C	29.7	33.6	10.0	5.4	98.7	99.2

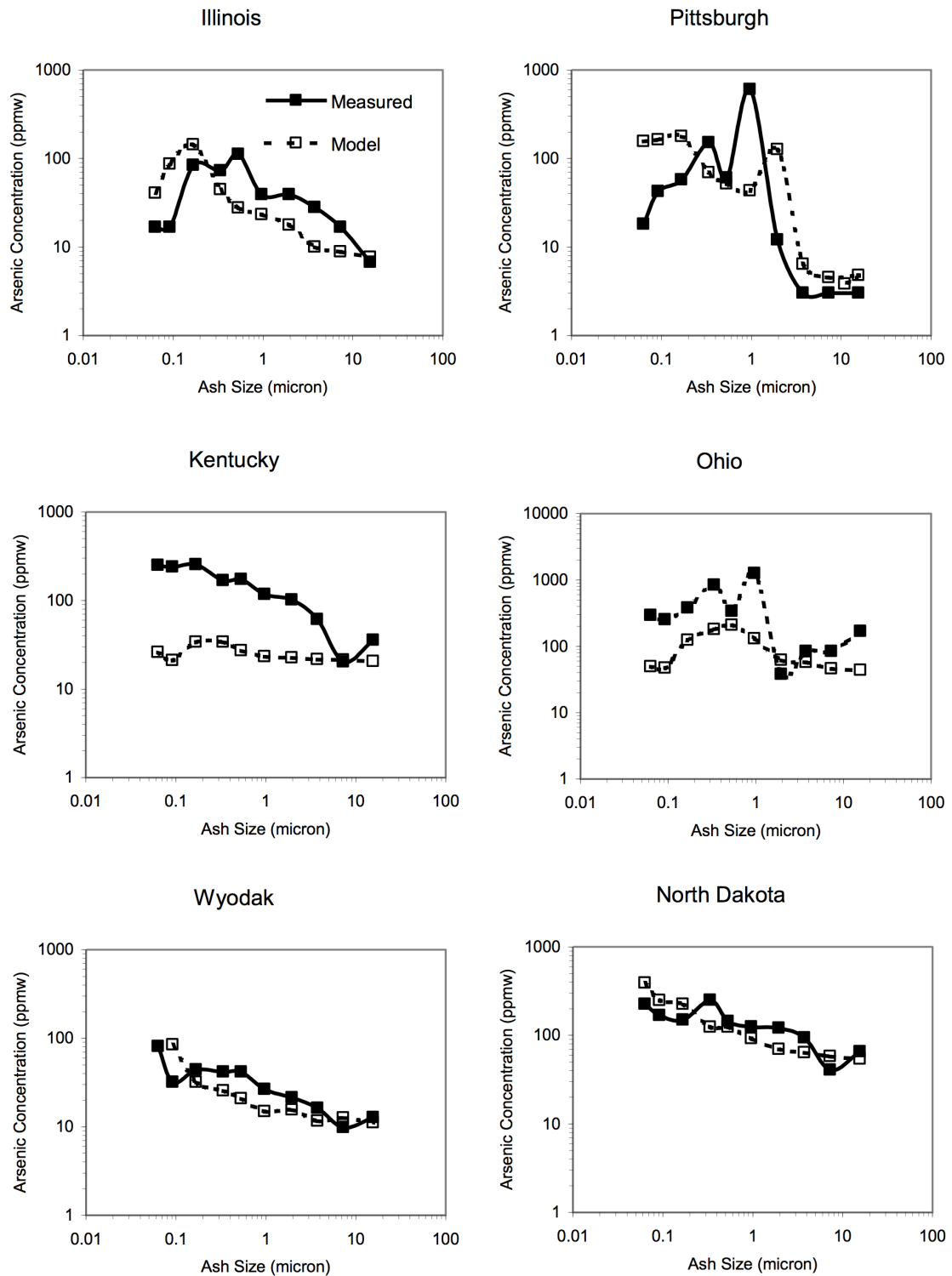


Figure 6: Arsenic concentration in ash as a function of particle diameter: measured and calculated values.

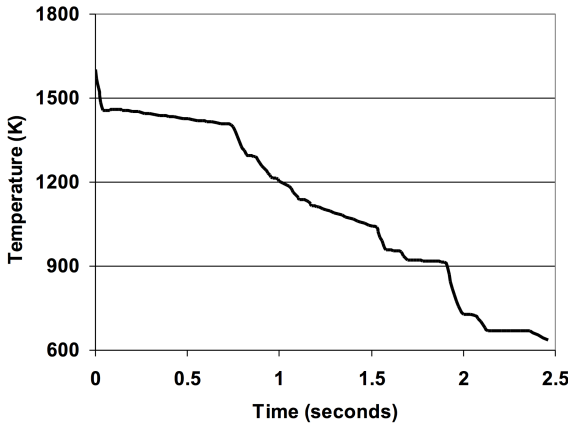
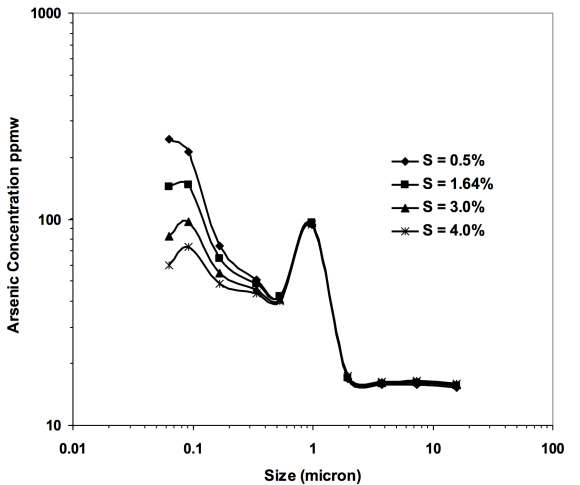


Figure 7: Boiler time-temperature history.



decreases. For the Pittsburgh coal, which has 4.6% CaO in the ash, the amount of the arsenic recovered by the ash (at 370 °C) varies from 43% at 0.5% sulfur (equivalent to a low-sulfur bituminous coal) to 26% at 4% sulfur (equivalent to a high-sulfur bituminous coal). The Kentucky coal is much lower in calcium, with little arsenic predicted to react with the ash. Thus, adding sulfur to this coal is not predicted to have a large impact on arsenic partitioning because little of the arsenic in the coal is expected to go into the particulate phase even when the sulfur content of the coal is low.

From Figs. 8 and 9, it is evident that the effect of sulfur concentration is manifested in the small particle sizes, below about 0.5  $\mu\text{m}$ . The smaller sizes have a higher flux of arsenic and SO<sub>2</sub> due to the higher surface area. Higher sulfur concentrations result in higher vapor arsenic concentrations and lower capture of vapor-phase arsenic by ash, as expected, due to lower CaO availability in high sulfur coals.

## 5. Conclusions

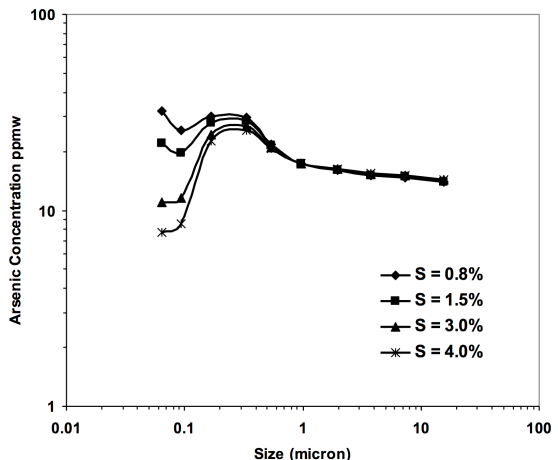
A model for arsenic partitioning in coal-fired boilers has been developed. The model predicts the partitioning of arsenic between the gas and solid phases in flue gas from coal-fired boilers, given the composition of the coal and the time-temperature history in the boiler. This model is intended to be used by utilities to help select, blend or test coals that minimize the amount of vapor-phase arsenic at economizer exit temperatures in order to prevent accelerated deactivation of SCR catalyst.

## Acknowledgements

Parts of this work were supported by the Department of Energy (Contract DE-AC22-95PC95101) and by EPRI (Project EP-P9714).

Sulfur in Coal, wt%	Predicted %As Capture by Fly Ash	Conc. As in Flame (ppbv)	Conc. As at Sampling Point (ppbv)
0.5%	42.9%	23	13
1.6%	33.6%	23	15
3.0%	28.1%	23	16.7
4.0%	25.6%	23	17.4

Figure 8: Effect of coal sulfur concentration on predicted arsenic in fly ash and in vapor phase at flame conditions (Initial) and at SCR inlet conditions (Final) for a full-scale boiler time-temperature history; baseline is Pittsburgh coal (4.6% CaO in ash).



Sulfur in Coal, wt%	Predicted %As Capture by Fly Ash	Conc. As in Flame (ppbv)	Conc. As at Sampling Point (ppbv)
0.8%	5.4%	23.3	22
1.5%	4.76%	23.4	22.3
3.0%	4.1%	23.6	22.6
4.0%	3.9%	23.8	22.8

Figure 9: Effect of coal sulfur concentration predicted arsenic in fly ash and in vapor phase at flame conditions (Initial) and at SCR inlet conditions (Final) for a full-scale boiler time-temperature history; baseline is Kentucky coal (2% CaO in ash).

## References

- [1] I. Morita, M. Hirano, G.T. Bielawski, Development and Commercial Operating Experience of SCR DeNOx Catalysts for Wet-Bottom Coal-Fired Boilers, presented at Power-Gen International Conference, Orlando, FL, December 8-11, 1998.
- [2] S.G. Pritchard, C.E. DeFrancesco, S. Kaneko, K. Suyama, Optimizing SCR Catalyst Design and Performance for Coal-Fired Boilers, presented at EPA/EPRI 1995 Joint Symposium on Stationary NOx Control, May 16-19, 1995, Electric Power Research Institute, 1995.
- [3] J.E. Staudt, T. Engelmeyer, W.H. Weston, R. Sigling, R., Deactivation of SCR Catalyst with Arsenic - Experience at OUC Stanton and Implications for Other Coal-Fired Boilers, presented at the Conference on Selective Catalytic Reduction (SCR) and Selective Non-Catalytic Reduction (SNCR) for NOx Control, Pittsburgh, Pennsylvania, May 15-16, 2002, US Department of Energy, National Energy Technology Laboratory, Pittsburgh, Pennsylvania, 2002.
- [4] T. Ake, C. Erickson, W. Medeiros, L. Hutcheson, M. Barger, S. Rutherford, Limestone Injection for Protection of SCR Catalyst, presented at the Mega-Symposium, Washington, D.C., May 19-22, 2003, Air & Waste Management Association, 2003.
- [5] F. Fransden, K. Dam-Johansen, P. Rasmussen, Trace Elements from Combustion and Gasification of CoalAn Equilibrium Approach, *Prog. Energy Combust.Sci.* 20 (1994) 115-138.
- [6] C.L. Senior, F. Huggins, G.P. Huffman, N. Shah, N. Yap, J.O.L. Went, W.S. Seames, III, M.R. Ames, A.F. Sarofim, S. Swenson, J.S. Lighty, A. Kolker, R. Finkelman, C.A. Palmer, S.J. Mroczkowski, J.J. Helble, R. Mamani-Paco, R. Sterling, G. Dunham, S. Miller, Toxic Substances from Coal Combustion A Comprehensive Assessment, Final Report, prepared for Department of Energy under Contract No. DE-AC22-95PC95101, PSIT-1283/TR-1745, Physical Sciences, Inc., Andover, Massachusetts, 2001.
- [7] J. D. Seader, and E. J. Henley, Separation Process Principles, John Wiley & Sons, Inc., New York, 1998.
- [8] S.G. Kang, J. Moore, J.J. Helble, S.A. Johnson, Utilization of Inherent Calcium in Near-Compliance Coals for Sulfur Capture, Final Report prepared for New England Power Service Company, Contract No. 2193, Physical Sciences, Inc., Andover, Massachusetts, 1992.
- [9] W.S. Seames, W.S., The Partitioning of Trace Elements During Pulverized Coal Combustion, PhD Dissertation, Appendix C, University of Arizona, Chemical and Environmental Engineering, 2000.
- [10] R.E. Hillamo, E.I. Kauppinen, *Aerosol Sci. Tech.* 14 (1991) 33-47.
- [11] Battelle, Columbus, Ohio, A Study of Toxic Emissions from a Coal-Fired Power PlantNiles Station Boiler No. 2, Final Report prepared for Department of Energy, under contract No. DE-AC22-93PC93251, Battelle, Columbus, Ohio , 1994.
- [12] Energy and Environmental Research Corporation, Assessment of Toxic Emissions from a coal Fired Power Plant Utilizing an ESP, Final Report, prepared for Department of Energy under contract No. DE-AC22-93PC93252, Energy and Environmental Research Corporation, Irvine, California, 1994.
- [13] Illinois Power Company, Toxic Assessment Report, Volume III, Appendix D, prepared for Department of Energy under Contract No. DE-AC2293PC93255, Illinois Power Company, Baldwin, Illinois, 1994.
- [14] Minnesota Power Company, Toxic Assessment Report, Volume I, prepared for Department of Energy under Contract No. DE-AC22-93PC93255, Minnesota Power Company, Cohasset, Minnesota, 1994.
- [15] Radian Corporation, A Study of Toxic Emissions from a Coal-Fired Power Plant Utilizing an ESP While Demonstrating the ICCT CT-121 FGD Project, Final Report, prepared for Department of Energy under contract No. DE-AC22-93PC93253, DCN 93-643-004-03, Radian Corporation, Austin, Texas, 1994.
- [16] Radian Corporation, PISCES Field Chemical Emissions Monitoring Project: Site 11 Emissions Report, Final Report, prepared for Electric Power Research Institute, under contract No. EPRI TR-105616, project 3177-01, Radian Corporation, Austin, Texas, 1995.
- [17] Radian Corporation, PISCES Field Chemical Emissions Monitoring Project: Site 21 Emissions Report, Final Report, prepared for Electric Power Research Institute, under contract No. EPRI TR-105625, project 3177-09, Radian Corporation, Austin, Texas 1995.
- [18] Southern Research Institute, Characterizing Toxic Emissions from a Coal-Fired Power Plant Demonstrating the AFGD ICCT Project and a Plant Utilizing a Dry Scrubber/Baghouse System, Springerville Generating Station Unit No. 2, Final Report, prepared for Department of Energy under contract No. DE-AC22-93PC93254, SRI Report No. SRI-ENV-94-476-7960, Southern Research Institute, Birmingham, Alabama, 1994.
- [19] Southern Research Institute, Characterizing Toxic Emissions from a Coal-Fired Power Plant Demonstrating the AFGD ICCT Project and a Plant Utilizing a Dry Scrubber/Baghouse System, Baily Station Units 7, 8, Final Report, prepared for Department of Energy under contract No. DE-AC22-93PC93254, SRI Report No. SRI-ENV-94-827-7960, Southern Research Institute, Birmingham, Alabama, 1994.